Express Polymer Letters Vol.16, No.9 (2022) 996–1010
Available online at www.expresspolymlett.com
https://doi.org/10.3144/expresspolymlett.2022.72

Research article

Creation of fully degradable poly(lactic acid) composite by using biosourced poly(4-hydroxybutyrate) as bioderived toughening additives

*Tianshu Zhang, Hao Wu, Huaping Wang, Abin Sun, Ze Kan**

Key Laboratory of Biobased Polymer Materials, Shandong Provincial Education Department, College of Polymer Science and Engineering, Qingdao University of Science and Technology, Qingdao, China

Received 14 February 2022; accepted in revised form 17 May 2022

Abstract. The inherent brittleness of poly(lactic acid) (PLA) limited its practical applications, so toughening modification was necessary. Poly(4-hydroxybutyrate) (P4HB) is fully biosourced and biodegradable polyester with the advantages of high strength and good toughness. In this study, P4HB was used to toughen PLA. The effects of composition, molecular weight, and processing method on the toughening of PLA were investigated. Tensile testing showed the elongation at failure of the PLA/P4HB composites increased with the increased P4HB content while the ultimate tensile strength gradually decreased. The composite containing 30% P4HB can offer a 40 times increase in elongation at failure compared with neat PLA. In the meantime, the ultimate tensile strength remained 48 MPa. Furthermore, the particle size and distribution of P4HB in PLA were tailored by changing the molecular weight and processing method to obtain a higher impact toughness. Importantly, there was a peak in impact strength (27 kJ/m^2) of the PLA/P4HB composites when the particle size of P4HB was in the range of 1.1–1.3 μm. This study provides not only a new toughener to prepare fully degradable PLA with high toughness and high strength but also sets up a universal framework for designing high-performance PLA products with suitable toughener particle sizes.

Keywords: *polymer blends and alloys, mechanical properties, processing technologies, biodegradable polymers*

1. Introduction

Poly(lactic acid) (PLA) has attracted extensive attention in recent years for its potential substitution of petroleum-based polymers [1–4]. Owing to its excellent renewability, biocompatibility, and processability, PLA displayed extensive applications, such as biomedical devices, packaging, and automotive industries [5, 6]. However, the inherent brittleness of PLA limited its practical applications, so toughing modification was necessary [6, 7]. Several types of toughener were applied to tough PLA, including plasticizers, nanoparticles, and polymers. For plasticizers, there was polyethylene glycol (PEG), citrate esters, *etc.* [8, 9]. However, this method will result in plasticizers migrating to the surface and a significant reduction in the strength of PLA. For nanoparticles, there was graphene oxide, silicon dioxide, *etc.* [10, 11]. However, the toughening of nanoparticles generally required grafting modification, so it was costly and unsuitable for large-scale production. For polymers, there were non-degradable polymers and degradable polymers. The use of compound poly(lactic acid) with non-degradable polymers, such as Polyethylene (PE), Polyolefin elastomer (POE), Nitrile-butadiene rubber (NBR), and Thermoplastic urethanes (TPU), could reduce brittleness at the expense of the degradability of the blend [12–15]. The ideal method would use a degradable flexible polymer to toughen PLA

*Corresponding author, e-mail: zkan@qust.edu.cn
© BME-PT

to create of fully degradable composite. Recently, poly(lactic acid) blended with other degradable flexible resins, such as Poly(butylene adipate-co-terephthalate) (PBAT), Polybutylene succinate (PBS), and Polycaprolactone (PCL), has been extensively studied [16–18]. These degradable polyesters have a low glass transition temperature and act like rubber at room temperature. The polyester particles dispersed in PLA cause stress concentration and cavitation when impacted [19, 20]. This cavitation initiates shear yielding, or crazing further develops to cause large plastic deformation of the matrix to dissipate a large amount of fracture energy [21]. Unfortunately, these degradable polymers also have problems such as low mechanical strength, high price, and poor compatibility with poly(lactic acid). Therefore, it is important to develop a high-performance degradable polymer to toughen PLA.

Polyhydroxyalkanoate (PHA) is a general term for a special class of aliphatic polyesters [22, 23]. Polyhydroxybutyrate (PHB) is the most common PHA; it has good biocompatibility, biodegradability, and non-toxicity. And it has a high degree of crystallinity (50–70%), its melting point is about 180 °C, and the glass transition temperature (T_g) is about 4 °C. Its mechanical properties are similar to those of polypropylene, the tensile strength is 25~35 MPa, and it also has good gas barrier properties. However, it also has many shortcomings, such as brittleness (elongation at break is less than 5–7%), poor thermal stability, high production cost, and low melt viscosity [22, 24–26]. Many researchers have also studied the PLA/PHB composites. For example, Zhang and Thomas [27] prepared PLA/PHB composites with different ratios by melt blending to investigate whether PHB could improve the heat distortion temperature and toughness of PLA. Olejnik *et al.* [28] also tried to study PLA/PHB composites with different ratios and found that with the increase of PHB content, the maximum tensile strength of the composites decreased continuously, while the elongation at break increased. In order to obtain high-performance composites, many researchers have adopted various modification methods, such as adding plasticizers [29, 30]. However, there are still many problems with this system for large-scale commercial applications. Poly(4-hydroxybutyrate) (P4HB) is a new generation product with good comprehensive performance and degradability among Polyhydroxyalkanoates (PHAs) materials, produced through microbial fermentation [31, 32]. P4HB can also be synthesized using a chemical method. The raw material γ-butyrolactone (γ-BL) can be obtained from biosource (*e.g.*, sugars). Our team used a self-developed binary catalytic system, overcoming the challenge of the ring-opening polymerization of five-membered ring lactones, to synthesize high molecular weight poly(γ-butyrolactone) that has mechanical properties similar to those of P4HB obtained by biological fermentation [33, 34] Chemical synthesis has been thought to be the most economical and effective route, as it can greatly reduce the cost of P4HB, promoting the application of P4HB in traditional plastic products. This biosourced P4HB is a thermoplastic semi-crystalline material with good mechanical properties: high strength (Tensile strength is 50–60 MPa) and good toughness (Elongation at break is 600–800% and Izod notched impact strength is about 60 kJ/m^2), indicating the promise in toughening PLA. This study mainly focuses on the structure and performance of the fully degradable PLA/P4HB composites affected by miscibility, composition, molecular weight, and processing. It is expected that the high toughness and strength of P4HB can be used to improve the brittle behavior of the PLA matrix while maintaining the high mechanical strength of the composites.

2. Experiments

2.1. Materials

The PLA (LX175, TotalEnergies Corbion, Netherlands) used in this study had a melt flow rate of 3 g/10 min (190 °C/2.16 kg). P4HB samples were synthesized via ROP of γ-BL with different weight-averaged molecular weights (M_w) of 158 kDa (P4HB-1), 109 kDa (P4HB-2), and 72.4 kDa (P4HB-3), the SEC traces of different P4HB were shown in Figure 1. Directly synthesized P4HB is an inhomogeneous lump. The bulk P4HB was hot-pressed at 80 °C into sheets and then cut to particles. Because many researchers have studied the PLA/PCL system and have obtained composite materials with high impact performance through various methods, and the structure of PCL is similar to that of P4HB, so PCL is selected as a reference object. Polycaprolactone (PCL) (1000C, Shenzhen Esun Industrial Co., China) was used in this study with a melt flow rate of 6 g/10 min (100 °C/2.16 kg).

2.2. Preparation of PLA/P4HB composites

PLA and P4HB granules with different viscosity (P4HB-1, P4HB-2, P4HB-3) were dried at 80 and

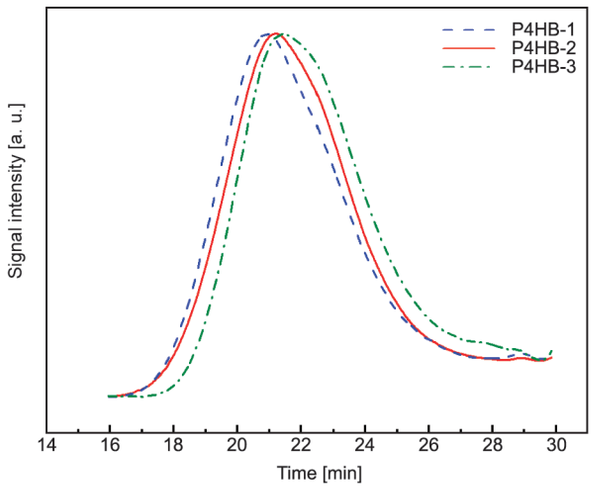

Figure 1. SEC traces of different P4HB, THF was used as the eluent at a flow rate of 1.0 ml/min at 40 °C.

45 °C for 4 and 8 h, respectively. Pure PLA and different PLA/P4HB-2 composites (90/10, 80/20, 70/30, and 60/40 mass ratio) were prepared using a torque rheometer RM-2000 (60 ml) (Harbin Harp Electrical Technology Co., Ltd., Harbin, China) blending for 10 min at 165 °C and a speed of 60 rpm. Tensile and impact samples were prepared by a Plate-press (BP-8170-A, Baopin Precision Instrument Co., Ltd., DongGuan, China) at 160 °C for 3 min and then pressed at 10 MPa for 5 min under the same temperature. The effect of the blending process on the structure and performance of PLA/P4HB-2 composites was investigated at three different torque speeds. To study the influence of the pressure and time of the molding process, PLA/P4HB-1, PLA/P4HB-2, PLA/P4HB-3 were prepared using a torque rheometer RM-2000 (60 ml) blending for 10 min at 165 °C, and a speed of 60 rpm and five different molding methods were adopted, four pressed with different pressures and time.

The injection samples were prepared by a miniature injection molding machine (WZS10D, Shanghai Xinshuo Precision Machinery Co., Ltd., China). The source material is held at a barrel temperature of 190 °C and then injected at a pressure of 0.4 MPa into the mold held at 30 °C. The pressure is held for 60 s to make sure the mold is filled. Table 1 summarizes the different molding methods.

2.3. Size exclusion chromatography (SEC)

Size exclusion chromatography (SEC) experiments were performed on an Agilent HPLC system (1260, Agilent, US) equipped with a Hip degasser (1260, Agilent, US), an Iso pump (1260, Agilent, US), and differential refractometer detector (1260, Agilent, US) with using tetrahydrofuran (THF) as mobile phase at a flow rate of 1.0 ml/min at 40 °C. One PLgel 5 µm guard column and three Mz-Gel SDplus columns (10^3–10^4 and 10^5 Å, the linear range of M_w = 1000–$2{\cdot}10^6$ Da) were connected in series. The molecular weight and dispersity were calculated using 6 polystyrene standards with narrow molecular weight distribution as references. The sample concentration used for SEC analyses was 5–10 mg/ml.

2.4. Differential scanning calorimetry (DSC)

Differential scanning calorimetry (DSC) measurements were performed on a differential scanning calorimeter (DSC 25,TA Instruments, US) under a N_2 atmosphere with a flow rate of 50 ml/min. Each sample weighed between 5~10 mg and was sealed individually in aluminum pans. The PLA/P4HB samples were heated from -80 to 200 °C for 2 cycles, and the P4HB samples were heated from –80 to 100 °C for 2 cycles. The heating and cooling rates were 10 °C/min.

2.5. Dynamic mechanical testing (DMA)

Dynamic mechanical analysis (DMA) was conducted to measure the evolution of the storage modulus (G') and the damping factor ($\tan\delta$) using a dynamic thermomechanical analysis (Q800,TA Instruments, US). Samples with a size of 40 mm× 10 mm×4 mm were subjected to a temperature program from –80 to 150 °C at a constant heating rate of 3 °C/min during a single cantilever mode mechanical test using a frequency of 1 Hz and an amplitude of 10 µm. The glass transition temperature

Table 1. Different molding methods.

Method	Forming method	Pressure [MPa]	Temperature [°C]	Time [min]
Method 1 (M1)	Compression	10.0	160	5
Method 2 (M2)	Compression	5.0	160	10
Method 3 (M3)	Compression	2.5	160	10
Method 4 (M4)	Compression	2.5	160	5
Method 5 (M5)	Injection	0.4	190	1

(T_g) was determined by the peak maximum of the damping factor curve.

2.6. Tensile testing

Tensile property measurements were conducted using a tensile tester (GF-HV2000A, GOTECH Testing Machines Inc., China)with a 1 kN load cell and a crosshead speed of 50 mm/min according to ISO 527. The testing specimens are 5A type (overall length l_3 = 75 mm, width at narrow portion b_1 = 4 mm, and thickness h = 2 mm) and were prepared by a plate-press as described in Section 2.2.

2.7. Notch impact testing

Notch impact testing was conducted according to ISO 180 using an Izod impact tester (GT-2045-MDN, GOTECH Testing Machines Inc., China). The pendulum work capacity is 1 J. The testing specimens (length L = 80 mm, width W = 10 mm, and thickness B = 4 mm) were prepared by a plate-press as described in Section 2.2. The notches (type A) with a depth of 2 mm and a tip radius of 250 μm were prepared using a V-knife.

2.8. Scanning electron microscope (SEM)

The morphologies of the fracture surfaces were observed by a scanning electron microscope (Quanta FEG 250, FEI, US). All samples were coated with a thin layer of gold (2–3 nm) prior to imaging. Cryogenic fracture surface samples were created after immersion in liquid nitrogen for 30 min. The impact fracture surface was also observed from notch impact tests. The Image-Pro Plus software was used to quantify the particle size of P4HB phase dispersed in the PLA matrix; for each specimen, at least 300 particles from several different SEM micrographs were measured, neglecting those particles with diameters smaller than 50 nm [35] The particle size distribution of P4HB domains was characterized by the weight-average particle size (d_w) and the particle size distribution parameter (σ). These two parameters can be expressed by Equations (1) and (2), where n_i is the number of P4HB particles with the apparent diameter of d_i. The parameter σ was used to characterize the dispersity (σ = 1 for the monodisperse system and σ > 1 for the polydisperse system) [35]:

$$d_w = \frac{\sum_{i=1}^{N} n_i d_i^2}{\sum_{i=1}^{N} n_i d_i} \tag{1}$$

$$\ln \sigma = \sqrt{\frac{\sum_{i=1}^{N} n_i \left(\ln d_i - \ln d_w\right)^2}{\sum_{i=1}^{N} n_i d_i}} \tag{2}$$

3. Results and discussion

3.1. Miscibility of PLA with P4HB

The miscibility of PLA and P4HB-2 was investigated using DSC and DMA analyses. The heating and cooling DSC traces are shown in Figure 2. The P4HB-2 homopolymer displayed a crystallization peak (T_c) at 17.5 °C during cooling curve and a melting peak (T_m) at 60 °C during heating curve. The PLA homopolymer displayed a melting peak at 150 °C in the heating curve. In the composites, with the addition of P4HB, the cold crystallization peak temperature (T_{cc}) of PLA shifted to a high temperature (The T_{cc} of pure PLA is 114.9 °C when the content of P4HB is 40%, and the $_{Tcc}$ of PLA is 120.8 °C), which indicated that P4HB would hinder the molecular chain movement of PLA. Simultaneously, PLA

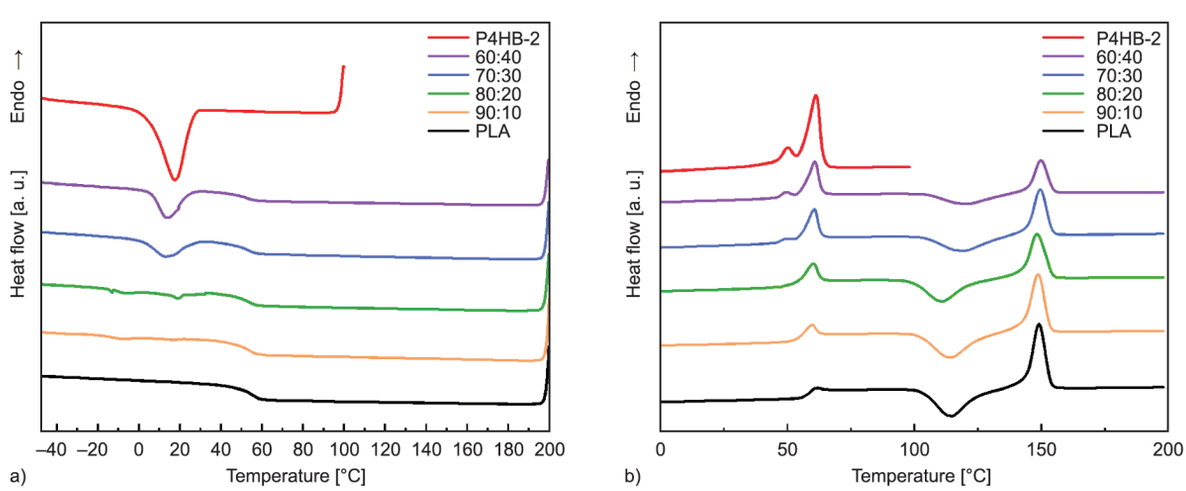

Figure 2. DSC cooling curves (a) and second heating curves (b) of PLA/P4HB-2 composites.

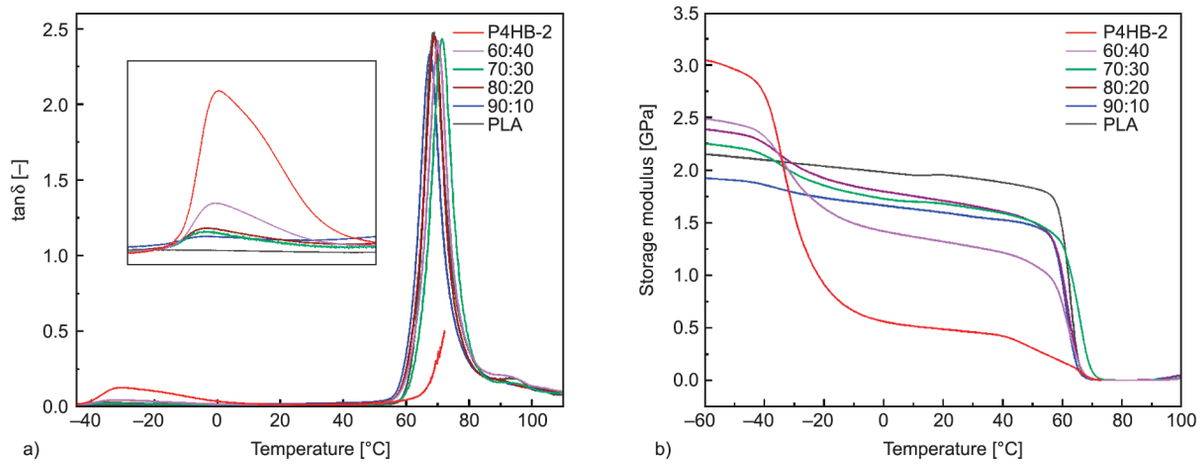

Figure 3. Tan δ (a) and storage modulus (b) of PLA/P4HB-2 composites.

inhibited the crystallization of P4HB-2. With the addition of PLA, the crystallization peak of P4HB broadened, and T_c shifted to a lower temperature (the T_c of pure P4HB is 17.5 °C, while the T_c of P4HB in the system of PLA/P4HB (90/10) is –8.0 °C). The DMA results in Figure 3 show two tan δ peaks that represent the glass transition temperature (T_g). The T_g of P4HB-2 was –30 °C, and the T_g of PLA was 70 °C. In the composites, the two peaks did not change significantly, indicating that they were incompatible. The curve of storage modulus versus temperature shows that P4HB-2 had a very high modulus when the temperature was lower than its T_g and decreased significantly above T_g. In the composites, this phenomenon was less pronounced, and the modulus of the composites was relatively stable below 60 °C.

3.2. Effect of composition of PLA/P4HB on the toughness

A series of PLA/P4HB composites with different compositions were prepared to explore the influence of P4HB content on the toughening of PLA. The tensile properties of PLA/P4HB-2 composites are shown in Figure 4 and Table 2. PLA exhibits brittle fracture. After adding P4HB-2, the composites exhibit obvious yield behavior and transform into a ductile fracture. The elongation at failure of the composites continued to increase with the increase in P4HB-2 content, with the ultimate tensile strength gradually decreasing. A 40 times increase in extension to failure was achieved with 30% P4HB-2 (165%) compared with PLA (4%) while retaining an ultimate tensile strength of 48 MPa.

Table 2. Young's modulus of PLA/P4HB-2 composites.

Component PLA/P4HB-2	Young's modulus [GPa]
100:0	15.8
90:10	13.2
80:20	12.2
70:30	11.6
60:40	6.2

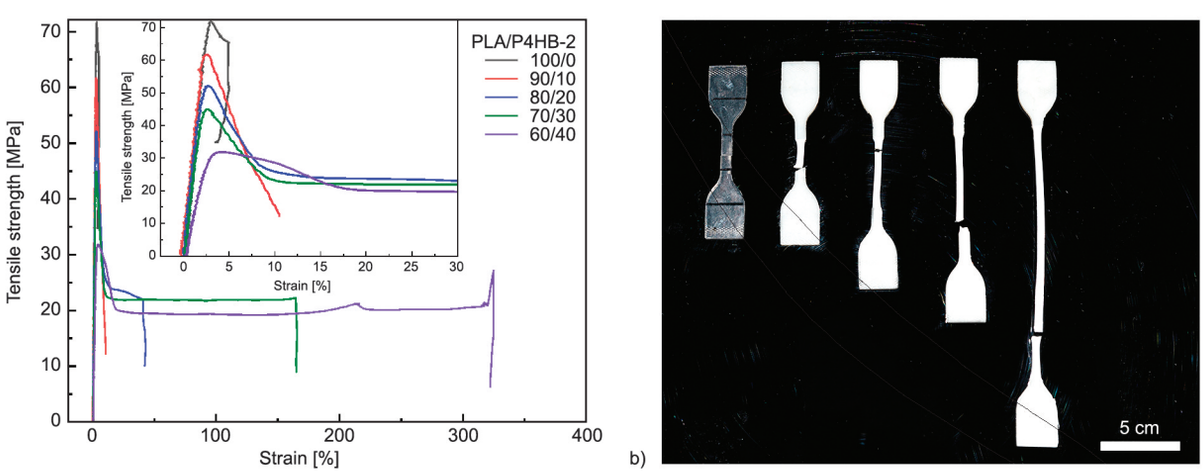

Figure 4. Stress–strain curves (a) and tensile samples of PLA/P4HB-2 composites (b).

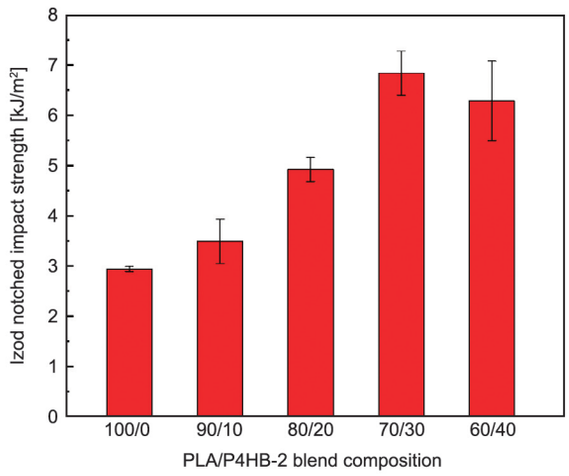

Figure 5. Impact strengths of PLA/P4HB-2 composites with different compositions.

Figure 5 shows the impact properties of PLA/P4HB-2 composites. The impact strength of composites increases with P4HB-2 content up to 30%; beyond that, it decreases slightly. This peak strength (P4HB-2 30%) of the composite was 6.8 kJ/m^2, double that of PLA.

These toughness improvements compared with PLA are less than those seen in other studies. The study of Bai *et al.* [35] suggests that the toughening effect was dependent on the particle size. If the particle size was too small, it would instigate crazing but not be able to arrest it and form cavities at the particle interface that develop into unstable cracks, both resulting in poor toughness. If the particle size was too large, the cracks would merge in the early stage of the impact test, leading to premature crack propagation and brittle fracture. All this suggests there is a window of particle sizes that maximizes the toughening effect by causing distributed crazing. The optimal particle size range of PCL toughened PLA has been reported as 1 μm [36, 37] Figure 6 shows the cryo-fracture surface of the 30% P4HB-2 sample illustrating the particles dispersed in the PLA phase. The particle size is measured from these images, with the data shown as a histogram in Figure 6. In the 30% P4HB-2 sample, the particle size was not uniform with particle size distribution parameter (σ) of 3.1 μm and the weight-average particle size (d_w) of 1.36 μm. This broad particle size distribution is suggested to be the limiting factor in the improvement in impact performance for the PLA/P4HB-2 composites. SEM images suggest that P4HB is more compatible with PLA than PCL. The interface between P4HB and PLA was less clear than that in the PLA/PCL case. Toughening PLA with PCL has been studied by many researchers [36–39] The molecular structures of P4HB and PCL are similar, indicating the promise of P4HB in toughening PLA.

Further, the particle size and distribution of P4HB in PLA would be tailored by changing the molecular weight and processing to obtain a higher impact toughness.

3.3. Effect of molecular weight of P4HB on the toughening of PLA

The viscosity of P4HB with different molecular weights is shown in Figure 7. The viscosity has an important impact on the particle size distribution of the composites during melt processing, which, in turn, affects the mechanical properties of the composites. Therefore, high (P4HB-1), medium (P4HB-2), and low (P4HB-3) molecular weights were selected. The

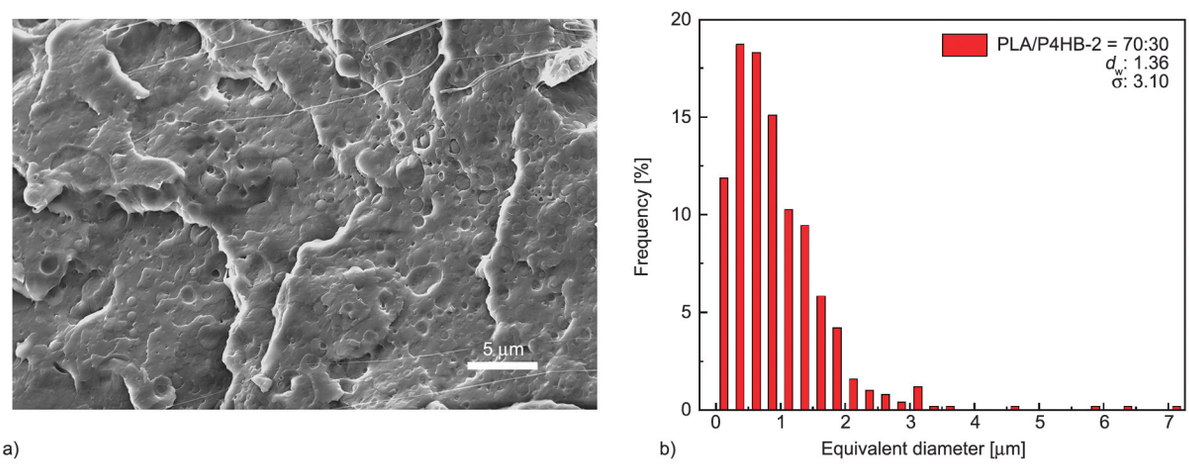

Figure 6. (a) SEM images of cryo-fractured surface morphology and (b) particle size distribution diagram of PLA/P4HB-2 (70/30).

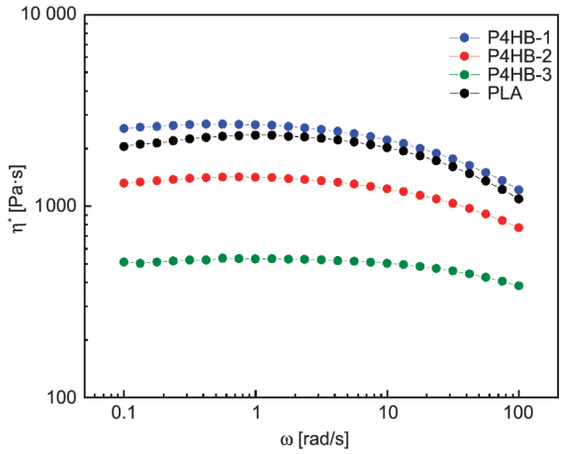

Figure 7. The shear viscosity of P4HB and PLA samples at 165 °C as a function of angular frequency.

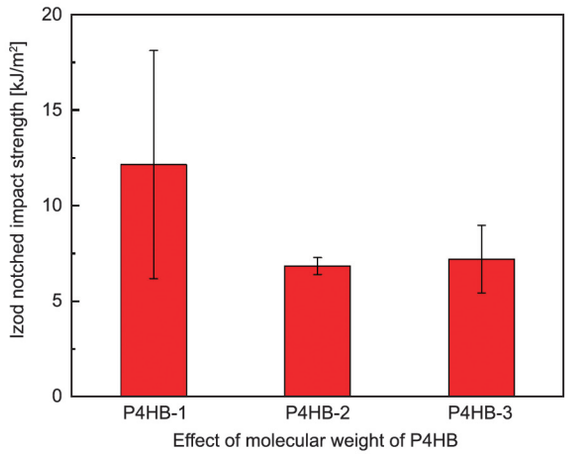

Figure 8. Impact strengths of PLA/P4HB (70/30) composites with different molecular weights.

impact strengths of the three composites are shown in Figure 8. The impact strength of PLA/P4HB-1 was up to 12 kJ/m^2 with a large standard deviation. The authors suggest this was related to the high viscosity of P4HB-1, leading to uneven blending. The impact strengths of PLA/P4HB-2 and PLA/P4HB-3 were similar, approximately 6 kJ/m^2. The influence of different molecular weights on the phase morphology of the composites is shown in the cryo-fracture surfaces and particle size of the composites. Figure 9 shows that the average particle size (d_w) of P4HB-1 in the composite was 1.62 μm with a narrow distribution index (σ), leading to high impact toughness. The d_w of P4HB-2 in the composite was 1.36 μm with a wide σ, leading to a small improvement in the impact toughness. The low impact toughness in P4HB-3 was attributed to the large d_w of 2.62 μm. This is because the viscosity of P4HB-3 was low, and the dispersed phase aggregated during the molding process. All this shows that different molecular weights of P4HB have different effects on the toughening of PLA due to the influence of the particle size and distribution of the dispersed phase.

We removed the SEM brittle fracture map in Figure 9 of the original manuscript and only retained the particle size distribution map.

3.4. Effect of processing on the toughening of PLA

To tailor the particle size and distribution of P4HB-2 in PLA, three different blending conditions were used (torque speeds of 40, 60, and 100 rpm). The particle

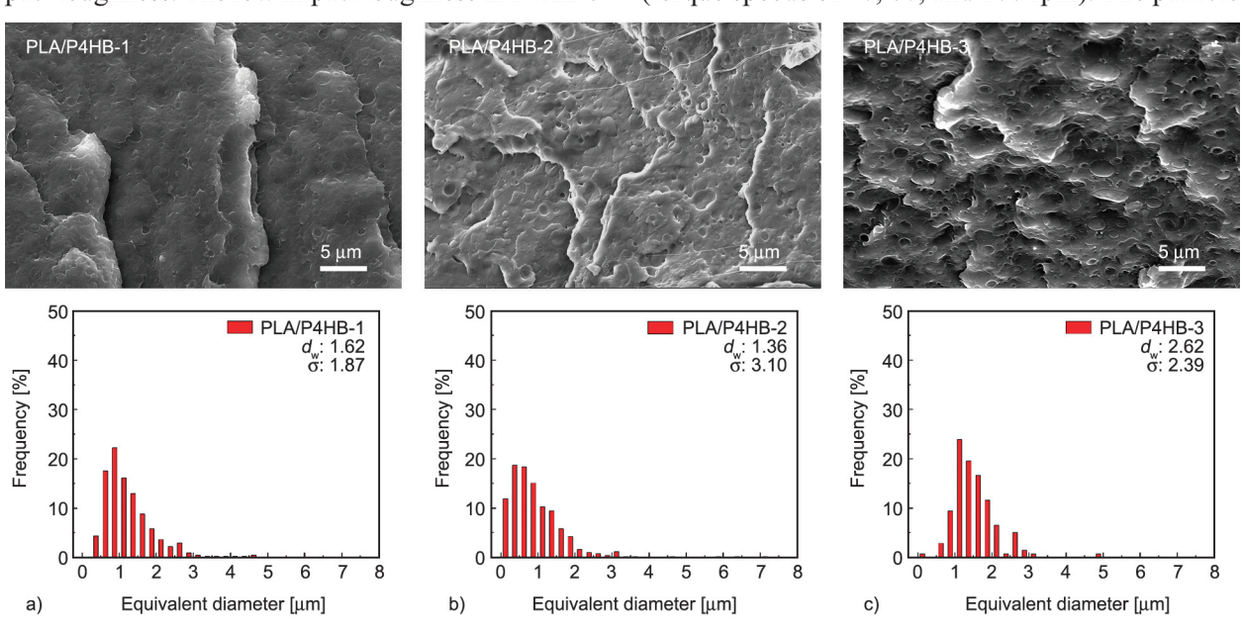

Figure 9. Particle size distribution diagram of PLA/P4HB (70/30) composites with different molecular weights. a) PLA/P4HB-1, b) PLA/P4HB-2, c) PLA/P4HB-3.

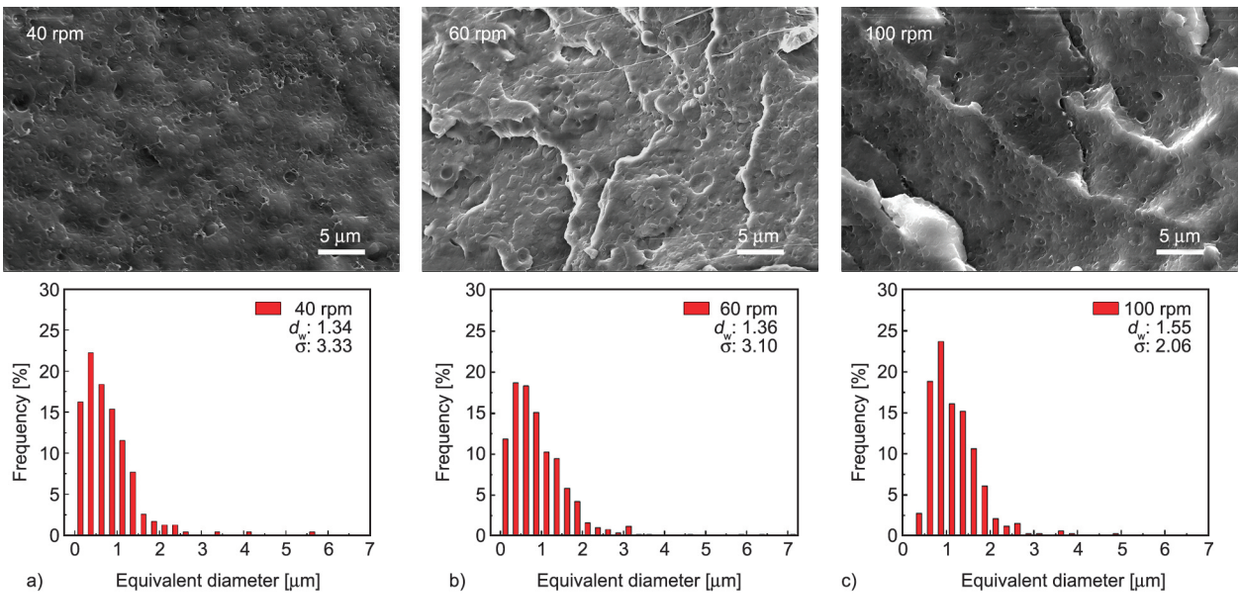

Figure 10. Particle size distribution diagram of PLA/P4HB (70/30) composites under different blending conditions. a) 40 rpm, b) 60 rpm, c) 100 rpm.

size distribution is shown in Figure 10. The d_w of P4HB-2 were similar during different torque speeds, and the σ for all were high. This led to little difference in the impact toughness (6.9, 6.8, and 6.7 kJ/m^2). The possible reason for no observed change in microstructure or toughness is due to the dominant effect of the molding pressure and time. The following section focuses on the influence of the molding process on the size and distribution of the dispersed phase.

We removed the SEM brittle fracture map in Figure 10 of the original manuscript and only retained the particle size distribution map.

An example of the change in the sample micromorphology during the molding process is shown in Figure 11. The d_w (0.36 µm) and σ (1.38 µm) of P4HB obtained before molding was small and uniform, respectively. The change during the molding is an increase in the particle size and a broadening of the distribution due to the external pressure and self-aggregation. This means that tailoring the molding pressure and time will result in composites with different P4HB particle sizes.

The impact strength and impact fracture surfaces of a series of composites prepared under the five molding conditions are shown in Figure 12 and Figure 13, respectively. This shows the impact strength of the PLA/ P4HB composites is significantly affected by the molding conditions. With the increase in the impact strength, the stress whitening phenomenon of the impact fracture surface became apparent, and the roughness of the fracture surface was increased. This was supported by the SEM images in Figure 13, showing that the cracks on the impact fracture surface were denser for samples with high impact strengths. The highest impact strength (27 kJ/m^2) was obtained using Method 3 (2.5 MPa, 10 min) and is

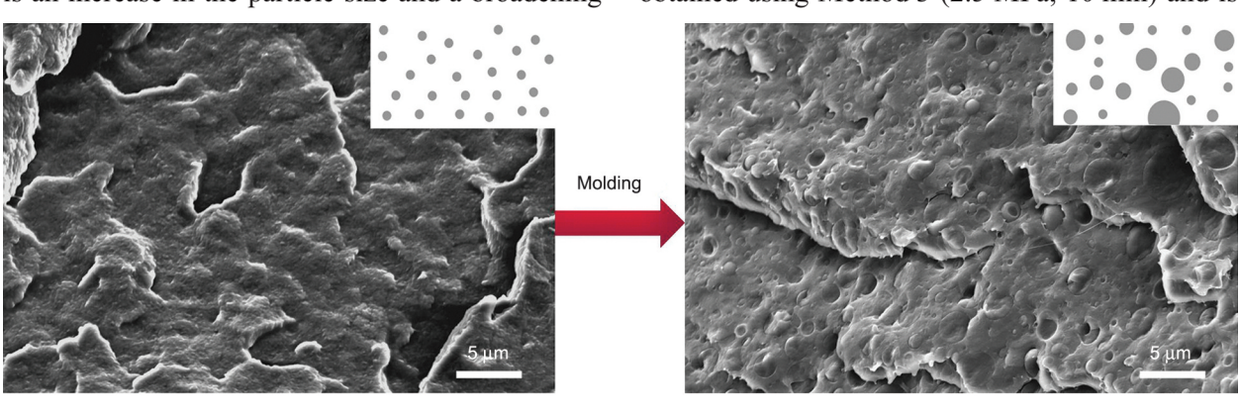

Figure 11. Schematic of the particle size change of PLA/ P4HB (70/30) composite a) before and b) after molding.

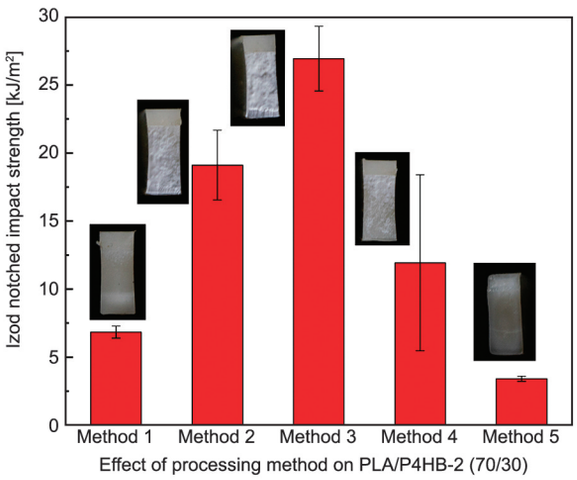

Figure 12. The Izod notched impact strengths of different molding processes for PLA/P4HB-2 (70/30) composites.

9 times greater than that of pure PLA. The second-highest impact strength was from Method 2 (5 MPa, 10 min) at 19 kJ/m^2.

The particle size distribution of P4HB under different molding conditions is obviously different, as shown in Figure 14. In Method 1, the P4HB aggregated seriously owing to the high molding pressure (10 MPa) and short molding time (5 min), leading to an uneven particle size of the dispersed phase and poor impact strength. Methods 2 and 3 reduced the molding pressure (5 and 2.5 MPa) and prolonged the molding time (10 min), giving d_w of 1.43 and 1.14 μm, respectively (both with small σ), leading to higher impact toughness. In Method 4, the molding pressure was 2.5 MPa with a reduced molding time (5 min). This reduces the d_w and σ to 0.97 and 1.37 μm, respectively. The impact strength for this method was 12 kJ/m^2, with a large standard deviation attributed to the short molding time. The d_w of the P4HB obtained in Method 5 was 0.47 μm, and the σ was 1.39 μm. This is because the injection pressure was low, and the molding time was short, meaning there was little self-aggregation of P4HB. In this case, the dispersed phase was too small to achieve a toughening effect. For all samples, a decrease in the molding pressure reduced the particle size and distribution of P4HB in the composites. Prolonging the molding time has been shown to make the particle size larger while narrowing the distribution. Urquijo *et al.* [40] also found similar results in the PLA/PCL system, but they did not obtain high-impact composites, which may be related to the too-small particle size of the PCL they obtained.

We removed the SEM brittle fracture map in Figure 14 of the original manuscript and only retained the particle size distribution map.

To explore the universality of these findings, the role of molding pressure and time were applied to the higher and lower molecular weight P4HB particles. The impact strengths for PLA/P4HB-1 and PLA/P4HB-3 under different molding conditions are shown in Figure 15. PLA/P4HB-1 using Method 1 gives an impact strength of 12 kJ/m^2 with Methods 4 and 5 as 9.8 and 4.1 kJ/m^2, respectively. The particle size distribution shown in Figure 16 illustrates that

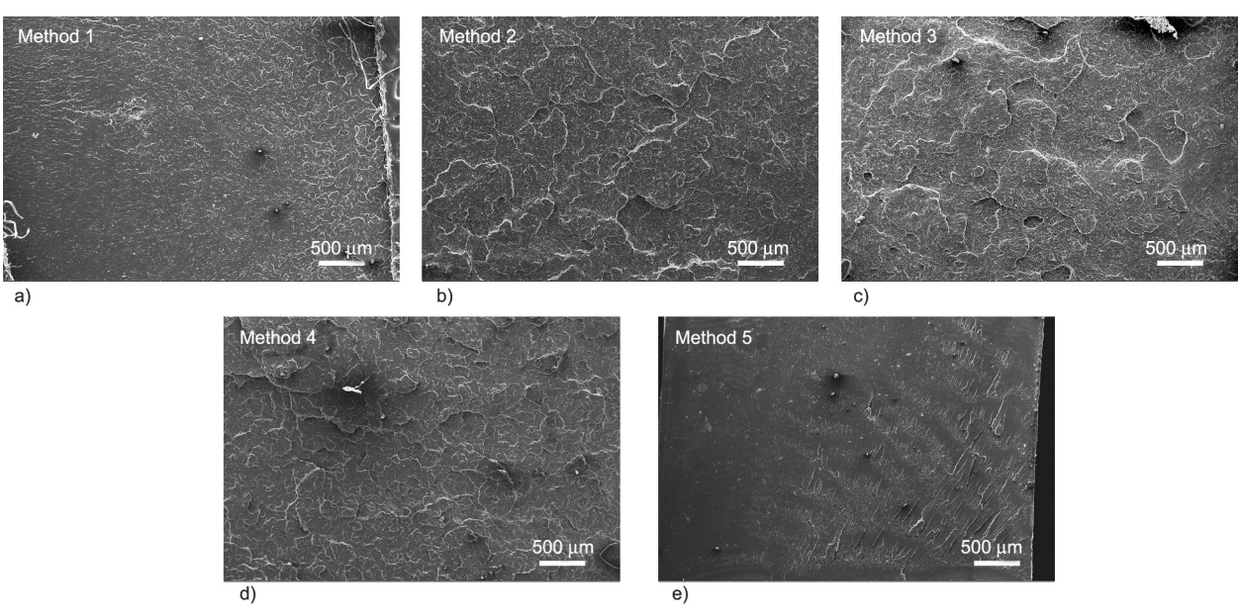

Figure 13. SEM images of impact fracture surfaces of different molding processes for PLA/P4HB-2 (70/30) composites. (a) Method 1, (b) Method 2, (c) Method 3, (d) Method 4, (e) Method 5.

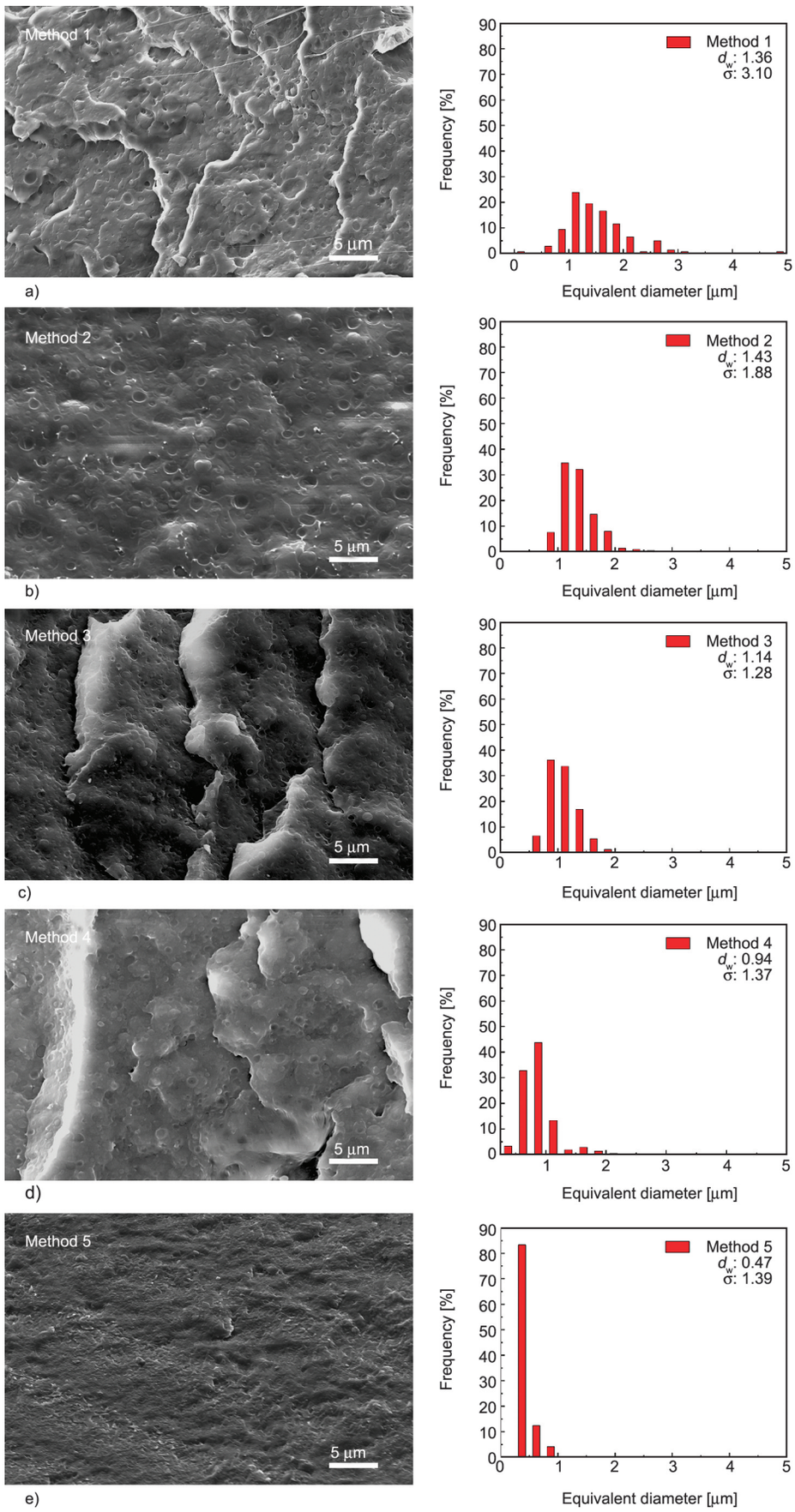

Figure 14. Particle size distribution diagram of PLA/P4HB-2 (70/30) composites under different molding processes. (a) Method 1, (b) Method 2, (c) Method 3, (d) Method 4, (e) Method 5.

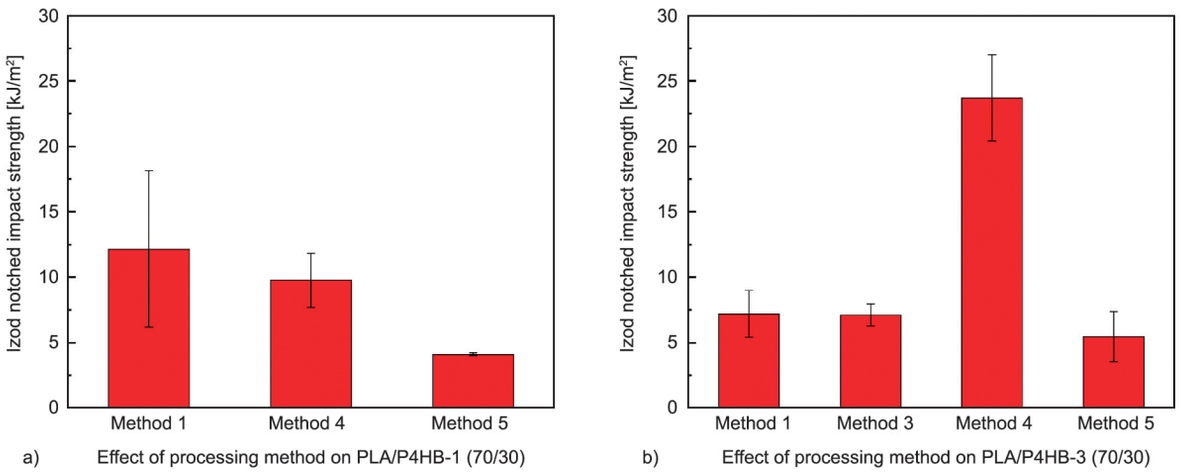

Figure 15. The Izod notched impact strengths of different molding conditions for a) PLA/P4HB-1 and b) PLA/P4HB-3 (70/30) composites.

the two different molding pressures of Methods 1 and 4 produced similar measures of dw, with σ being larger under the low pressure (Method 4 – 2.5MPa). This is because the viscosity of P4HB-1 is large, meaning the molding pressure in this range has little effect on phase structures. That is also why M2 and M3 were not included in this study. PLA/P4HB-3 had the greatest impact strength (24 kJ/m^2) using Method 4. The impact strengths prepared by Method 1, 3, and 5 were 7.2, 7.1, and 5.5 kJ/m^2, respectively. The P4HB particle size and distribution shown in Figure 17 suggest that the molding pressure had a significant influence on the particle size of the dispersed phase due to the low viscosity of P4HB-3. Prolonging the molding time (Method 4 – 5 min and Method 3 – 10 min) under the same pressure significantly increased the particle size of the dispersed phase (1.33 and 2.22 μm), leading to a non-uniform particle size distribution. Comparing the structure and performance of PLA/P4HB composites with different viscosities suggests that P4HB-2 performed best. The viscosity of P4HB-2 being slightly lower than that of PLA allowed for the smallest particle size of the dispersed phase and controlled size within a wide range via changing molding pressure and molding time.

We removed the SEM brittle fracture map in Figures 16 and 17 of the original manuscript and only retained the particle size distribution map.

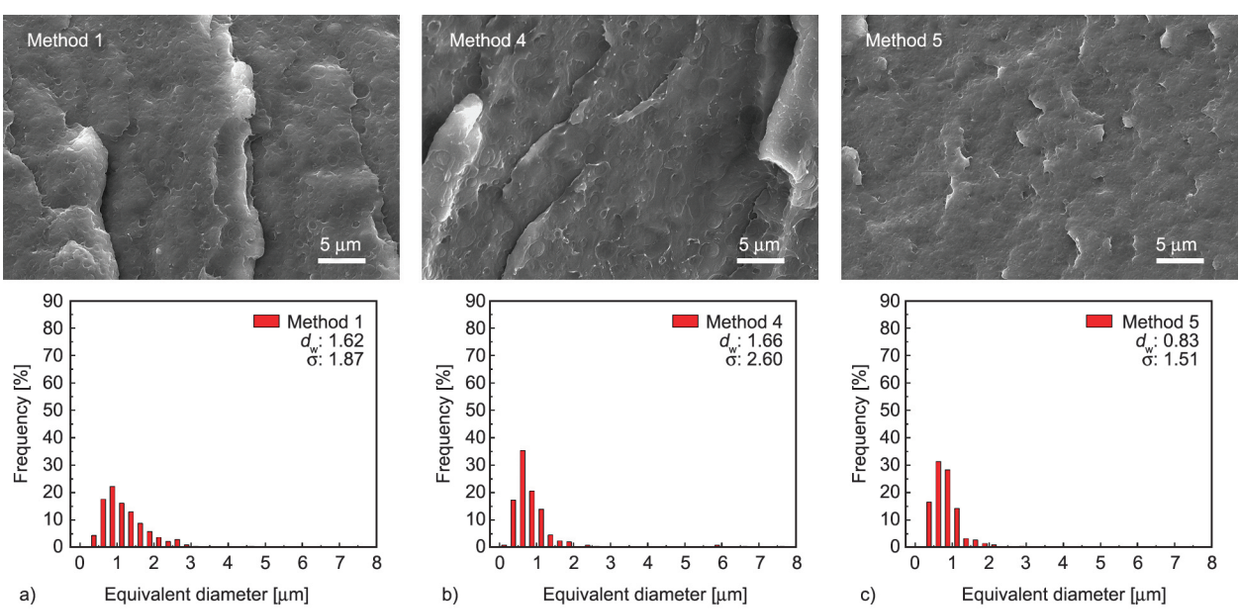

Figure 16. Particle size distribution diagram of PLA/P4HB-1 (70/30) composites prepared by different molding processes. a) Method 1, b) Method 4, c) Method 5.

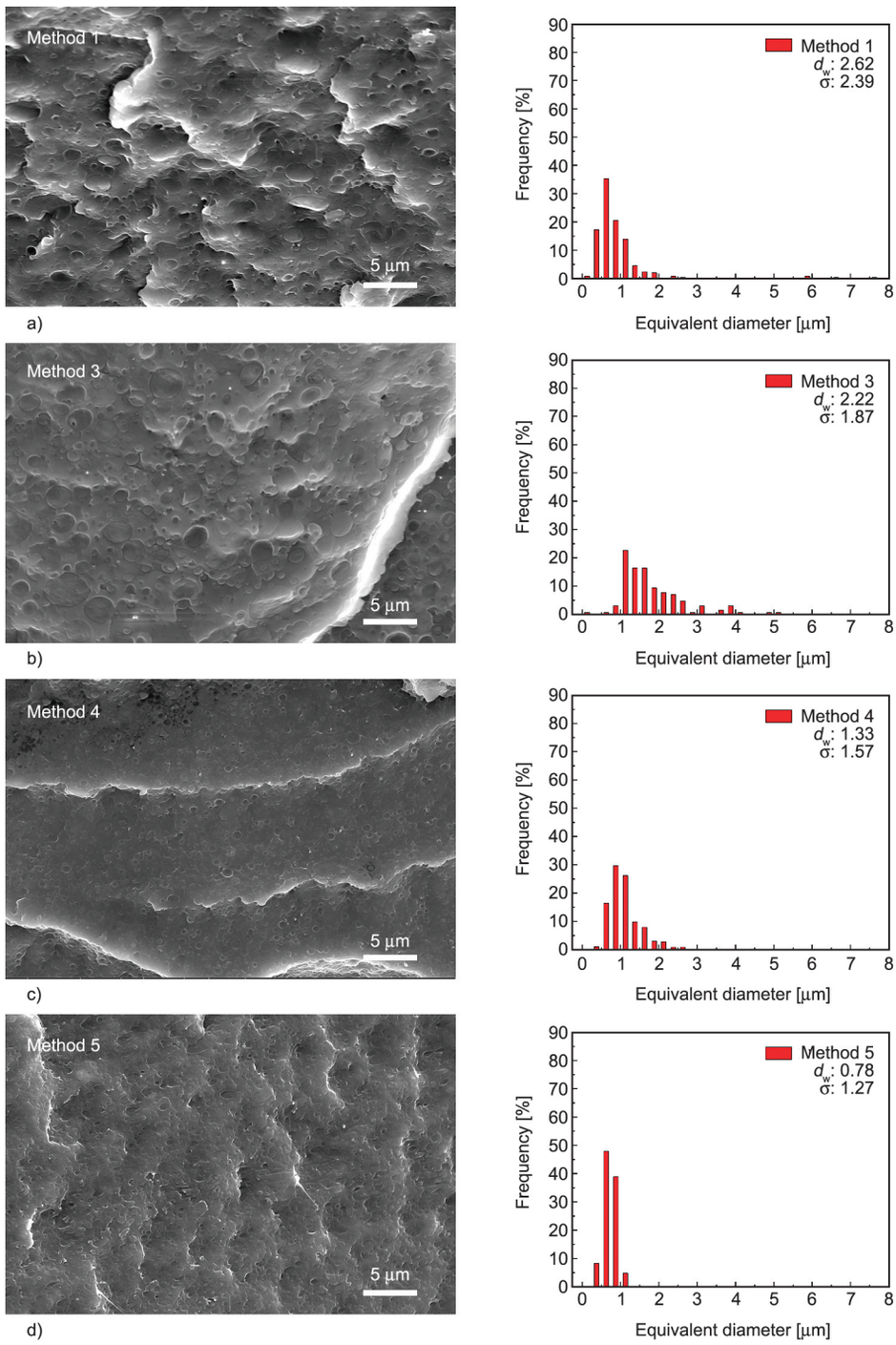

Figure 17. Particle size distribution diagram of PLA/P4HB-3 (70/30) composites under different molding processes. a) Method 1, b) Method 3, c) Method 4, d) Method 5.

3.5. Toughening mechanism

Combining the results above by taking the particle size of P4HB as the abscissa and the impact strengths of the composites as the ordinate, the relationship curve between particle size and impact strength was drawn and is shown in Figure 18. This illustrates that there is a peak in Izod notched impact strength of the PLA/P4HB composites when the particle size of P4HB was in the range of 1.1–1.3 µm. The authors suggest that this relationship with the particle size is owing to the mechanism of P4HB toughening PLA. With a smaller size, the particles will be subsumed by the crazing of the matrix around them and will not be able to stop the crazing from progressing through the material. This gives a low impact strength of the composite when the particle size of P4HB is less than 1.1 µm. When the particle size of P4HB is larger, it will cause unstable cracks. These cracks are

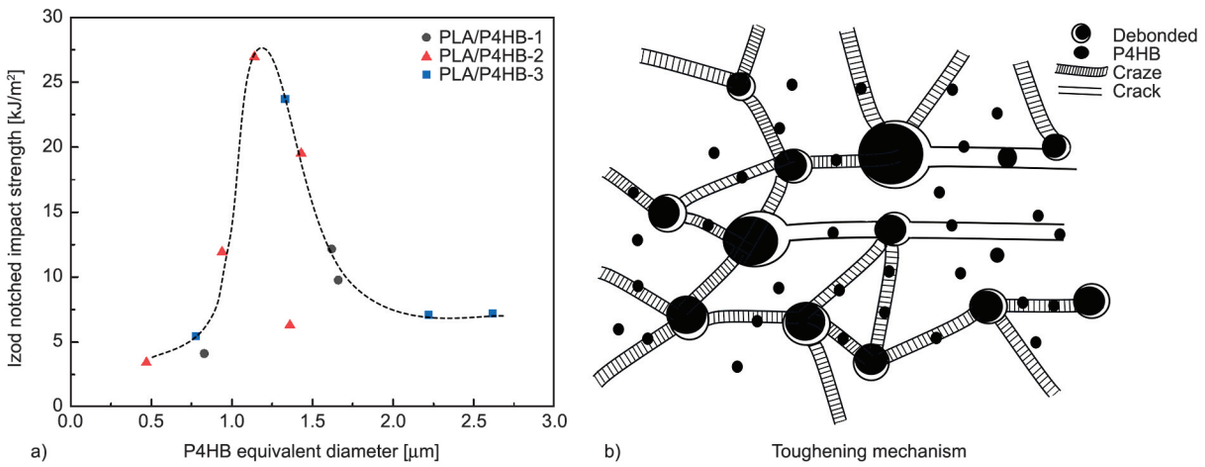

Figure 18. a) Relationship between P4HB particle size and impact strength and b) the mechanism of different particle sizes of P4HB in toughening PLA.

difficult to terminate and lead to rapid fracture of the matrix. This explains the rapid drop in impact performance when the particle size of P4HB is larger than 1.3 μm. When the P4HB particle size is in the range of 1.1–1.3 μm, it causes a mixture of failure mechanisms that interact and compete (Figure 18), thereby achieving a good toughening effect.

4. Conclusions

This study concludes that the PLA/P4HB composite has the highest tensile strength and elongation at failure and excellent impact performance when the P4HB content is 30%. We have shown that the molding process has a significant effect on the toughening of PLA, as it tailors the particle size and distribution of P4HB in PLA/P4HB composites. Due to the uniformly dispersed small P4HB particles in melt blending, they continue to agglomerate in the melt form during the molding process. With the extension of the molding time and the increase of the pressure, the agglomeration effect is continuously enhanced, and the particles of P4HB in the composite material continue to increase. These are easiest to adjust through the molding process when the viscosity of P4HB is slightly lower than that of PLA. A dispersed phase particle size ranging from 0.47 to 2.62 μm has been demonstrated by adjusting different molding processes. The toughening effect is shown to be at maximum when the particle size is in the range of 1.1–1.3 μm. The role of P4HB with different particle sizes in the toughening mechanisms has been discussed, providing a theoretical basis for the toughening of PLA by P4HB.

Acknowledgements

This work was supported by the National Natural Science Foundation of China (No. 51803104) and the 111 Project (No. D17004). Gratefully acknowledge our colleagues, Prof. Zhibo Li, and Dr. Yong Shen, for providing us with enough P4HB samples. The authors also acknowledge the very useful comments of Prof. Zhibo Li.

References

[1] Jamshidian M., Tehrany E. A., Imran M., Jacquot M., Desobry S.: Poly-lactic acid: Production, applications, nanocomposites, and release studies. Comprehensive Reviews in Food Science and Food Safety, **5**, 552–571 (2010). https://doi.org/10.1111/j.1541-4337.2010.00126.x

[2] Nampoothiri K. M., Nair N. R., John R. P.: An overview of the recent developments in polylactide (PLA) research. Bioresource Technology, **101**, 8493–8501 (2010). https://doi.org/10.1016/j.biortech.2010.05.092

[3] Atthoff B., Hilborn J.: Protein adsorption onto polyester surfaces: Is there a need for surface activation? Journal of Biomedical Materials Research Part B: Applied Biomaterials, **80**, 121–130 (2007). https://doi.org/10.1002/jbm.b.30576

[4] Auras R., Harte B., Selke S.: An overview of polylactides as packaging materials. Macromolecular Bioscience, **4**, 835–864 (2004). https://doi.org/10.1002/mabi.200400043

[5] Anderson K. S., Schreck K. M., Hillmyer M. A.: Toughening polylactide. Polymer Reviews, **48**, 85–108 (2008). https://doi.org/10.1080/15583720701834216

[6] Liu H., Zhang J.: Research progress in toughening modification of poly(lactic acid). Journal of Polymer Science Part B: Polymer Physics, **49**, 1051–1083 (2011). https://doi.org/10.1002/polb.22283

[7] Nofar M., Sacligil D., Carreau P., Kamal M. R., Heuzey M-C.: Poly(lactic acid) blends: Processing, properties and applications. International Journal of Biological Macromolecules, **125**, 307–360 (2019). https://doi.org/10.1016/j.ijbiomac.2018.12.002

[8] Feng X., Zhang S., Zhu S., Han K., Jiao M., Song J., Ma Y., Yu M.: Study on biocompatible PLLA-PEG blends with high toughness and strength *via* pressure-induced-flow processing. RSC Advances, **3**, 11738–11744 (2013). https://doi.org/10.1039/c3ra40899j

[9] Yang Z., Bi H., Bi Y., Rodrigue D., Xu M., Feng X.: Comparison between polyethylene glycol and tributyl citrate to modify the properties of wood fiber/polylactic acid biocomposites. Polymer Composites, **40**, 1384–71394 (2019). https://doi.org/10.1002/pc.24872

[10] Campos J. M., Ferraria A. M., do Rego A. M. B., Ribeiro M. R., Barros-Timmons A.: Studies on PLA grafting onto graphene oxide and its effect on the ensuing composite films. Materials Chemistry and Physics, **166**, 122–132 (2015). https://doi.org/10.1016/j.matchemphys.2015.09.036

[11] Wang B., Zhang X., Zhang L., Feng Y., Liu C., Shen C.: Simultaneously reinforcing and toughening poly (lactic acid) by incorporating reactive melt-functionalized silica nanoparticles. Journal of Applied Polymer Science, **137**, 48834 (2020). https://doi.org/10.1002/app.48834

[12] Anderson K. S., Lim S. H., Hillmyer M. A.: Toughening of polylactide by melt blending with linear low-density polyethylene. Journal of Applied Polymer Science, **89**, 3757–3768 (2003). https://doi.org/10.1002/app.12462

[13] Su Z., Li Q., Liu Y., Hu G-H., Wu C.: Compatibility and phase structure of binary blends of poly(lactic acid) and glycidyl methacrylate grafted poly(ethylene octane). European Polymer Journal, **45**, 2428–2433 (2009). https://doi.org/10.1016/j.eurpolymj.2009.04.028

[14] Han D-H., Choi M-C., Jeong J-H., Choi K-M., Kim H-S.: Properties of acrylonitrile butadiene rubber (NBR)/poly(lactic acid) (PLA) blends and their foams. Composite Interfaces, **23**, 771–780 (2016). https://doi.org/10.1080/09276440.2016.1170518

[15] Mo X-Z., Wei F-X., Tan D-F., Pang J-Y., Lan C-B.: The compatibilization of PLA-*g*-TPU graft copolymer on polylactide/thermoplastic polyurethane blends. Journal of Polymer Research, **27**, 33 (2020). https://doi.org/10.1007/s10965-019-1999-7

[16] Su S., Duhme M., Kopitzky R.: Uncompatibilized PBAT/PLA blends: Manufacturability, miscibility and properties. Materials, **13**, 4897 (2020). https://doi.org/10.3390/ma13214897

[17] Zhang X., Wang X.: Effect of carboxylic acid nucleating agent on crystallization and mechanical properties of PLA/PBS blends. Polymer Science Series A, **60**, 332–341 (2018). https://doi.org/10.1134/s0965545x18030185

[18] Sun H., Xiao A., Yu B., Bhat G., Zhu F.: Effect of PCL and compatibilizer on the tensile and barrier properties of PLA/PCL films. Polymer Korea, **41**, 181–188 (2017). https://doi.org/10.7317/pk.2017.41.2.181

[19] Nomai J., Jarapanyacheep R., Jarukumjorn K.: Mechanical, thermal, and morphological properties of sawdust/poly(lactic acid) composites: Effects of alkali treatment and poly(butylene adipate-*co*-terephthalate) content. Macromolecular Symposia, **354**, 244–250 (2015). https://doi.org/10.1002/masy.201400120

[20] Panda B. P., Mohanty S., Nayak S. K.: Mechanism of toughening in rubber toughened polyolefin-A review. Polymer-Plastics Technology and Engineering, **54**, 462–473 (2015). https://doi.org/10.1080/03602559.2014.958777

[21] Wang M., Wu Y., Li Y-D., Zeng J-B.: Progress in toughening poly(lactic acid) with renewable polymers. Polymer Reviews, **57**, 557–593 (2017). https://doi.org/10.1080/15583724.2017.1287726

[22] Bugnicourt E., Cinelli P., Lazzeri A., Alvarez V.: Polyhydroxyalkanoate (PHA): Review of synthesis, characteristics, processing and potential applications in packaging. Express Polymer Letters, **8**, 791–808 (2014). https://doi.org/10.3144/expresspolymlett.2014.82

[23] Meereboer K. W., Misra M., Mohanty A. K.: Review of recent advances in the biodegradability of polyhydroxyalkanoate (PHA) bioplastics and their composites. Green Chemistry, **22**, 5519–5558 (2020). https://doi.org/10.1039/d0gc01647k

[24] Raza Z. A., Noor S., Khalil S.: Recent developments in the synthesis of poly(hydroxybutyrate) based biocomposites. Biotechnology Progress, **35**, e2855 (2019). https://doi.org/10.1002/btpr.2855

[25] de O. Patrício P. S., Pereira F. V., dos Santos M. C., de Souza P. P., Roa J. P. B., Orefice R. L.: Increasing the elongation at break of polyhydroxybutyrate biopolymer: Effect of cellulose nanowhiskers on mechanical and thermal properties. Journal of Applied Polymer Science, **127**, 3613–3621 (2013). https://doi.org/10.1002/app.37811

[26] El-Hadi A., Schnabel R., Straube E., Müller G., Henning S.: Correlation between degree of crystallinity, morphology, glass temperature, mechanical properties and biodegradation of poly(3-hydroxyalkanoate) PHAs and their blends. Polymer Testing, **21**, 665–674 (2002). https://doi.org/10.1016/S0142-9418(01)00142-8

[27] Zhang M., Thomas N. L.: Blending polylactic acid with polyhydroxybutyrate: The effect on thermal, mechanical, and biodegradation properties. Advances in Polymer Technology, **30**, 67–79 (2011). https://doi.org/10.1002/adv.20235

[28] Olejnik O., Masek A., Zawadziłło J.: Processability and mechanical properties of thermoplastic polylactide/polyhydroxybutyrate (PLA/PHB) bioblends. Materials, **14**, 898 (2021). https://doi.org/10.3390/ma14040898

[29] Iglesias Montes M. L., D'amico D. A., Manfredi L. B., Cyras V. P.: Effect of natural glyceryl tributyrate as plasticizer and compatibilizer on the performance of bio-based polylactic acid/poly(3-hydroxybutyrate) blends. Journal of Polymers and the Environment, **27**, 1429–1438 (2019).
https://doi.org/10.1007/s10924-019-01425-y

[30] Wang B., Jin Y., Kang K., Yang N., Weng Y., Huang Z., Men S.: Investigation on compatibility of PLA/PBAT blends modified by epoxy-terminated branched polymers through chemical micro-crosslinking. e-Polymers, **20**, 39–54 (2020).
https://doi.org/10.1515/epoly-2020-0005

[31] Le Meur S., Zinn M., Egli T., Thöny-Meyer L., Ren Q.: Poly(4-hydroxybutyrate) (P4HB) production in recombinant *Escherichia coli:* P4HB synthesis is uncoupled with cell growth. Microbial Cell Factories, **12**, 123 (2013).
https://doi.org/10.1186/1475-2859-12-123

[32] Le Meur S., Zinn M., Egli T., Thöny-Meyer L., Ren Q.: Improved productivity of poly (4-hydroxybutyrate) (P4HB) in recombinant escherichia coli using glycerol as the growth substrate with fed-batch culture. Microbial Cell Factories, **13**, 131 (2014).
https://doi.org/10.1186/s12934-014-0131-2

[33] Shen Y., Zhao Z., Li Y., Liu S., Liu F., Li Z.: A facile method to prepare high molecular weight bio-renewable poly(γ-butyrolactone) using a strong base/urea binary synergistic catalytic system. Polymer Chemistry, **10**, 1231–1237 (2019).
https://doi.org/10.1039/C8PY01812J

[34] Zhao N., Ren C., Li H., Li Y., Liu S., Li Z.: Selective ring-opening polymerization of non-strained γ-butyrolactone catalyzed by a cyclic trimeric phosphazene base. Angewandte Chemie International Edition, **42**, 13167–13170 (2017).
https://doi.org/10.1002/ange.201707122

[35] Bai H., Huang C., Xiu H., Gao Y., Zhang Q., Fu Q.: Toughening of poly(L-lactide) with poly(ε-caprolactone): Combined effects of matrix crystallization and impact modifier particle size. Polymer, **54**, 5257–5266 (2013).
https://doi.org/10.1016/j.polymer.2013.07.051

[36] Ostafinska A., Fortelný I., Hodan J., Krejčíková S., Nevoralová M., Kredatusová J., Kruliš Z., Kotek J., Šlouf M.: Strong synergistic effects in PLA/PCL blends: Impact of PLA matrix viscosity. Journal of the Mechanical Behavior of Biomedical Materials, **69**, 229–241 (2017).
https://doi.org/10.1016/j.jmbbm.2017.01.015

[37] Fortelny I., Ujcic A., Fambri L., Slouf M.: Phase structure, compatibility, and toughness of PLA/PCL blends: A review. Frontiers in Materials, **6**, 206 (2019).
https://doi.org/10.3389/fmats.2019.00206

[38] Ostafinska A., Fortelny I., Nevoralova M., Hodan J., Kredatusova J., Slouf M.: Synergistic effects in mechanical properties of PLA/PCL blends with optimized composition, processing, and morphology. RSC Advances, **5**, 98971–98982 (2015).
https://doi.org/10.1039/C5RA21178F

[39] Ferri J. M., Fenollar O., Jorda-Vilaplana A., García-Sanoguera D., Balart R.: Effect of miscibility on mechanical and thermal properties of poly(lactic acid)/polycaprolactone blends. Polymer International, **65**, 453–463 (2016).
https://doi.org/10.1002/pi.5079

[40] Urquijo J., Guerrica-Echevarría G., Eguiazábal J. I.: Melt processed PLA/PCL blends: Effect of processing method on phase structure, morphology, and mechanical properties. Journal of Applied Polymer Science, **132**, 42641 (2015).
https://doi.org/10.1002/app.42641